

Parametric Landau damping of space charge modes

Alexandru Macridin, Alexey Burov, Eric Stern, James Amundson, Panagiotis Spentzouris
Fermilab, P.O. Box 500, Batavia, Illinois 60510, USA

Landau damping is the mechanism of plasma and beam stabilization; it arises through energy transfer from collective modes to the incoherent motion of resonant particles. Normally this resonance requires the resonant particle's frequency to match the collective mode frequency. We have identified an important new damping mechanism, *parametric Landau damping*, which is driven by the modulation of the mode-particle interaction. This opens new possibilities for stability control through manipulation of both particle and mode-particle coupling spectra. We demonstrate the existence of parametric Landau damping in a simulation of transverse coherent modes of bunched accelerator beams with space charge.

Introduction Landau damping (LD) [1] gives rise to the stabilization of collective modes in plasma and accelerator beams. The damping is caused by the energy transfer from the collective mode to the particles in resonance with the mode. The damping rate is, therefore, determined by the number of the particles capable of resonating with the mode. Conventionally, LD requires the coherent resonance frequency to lie within the incoherent spectrum, *i.e.*, the continuous frequency spectrum of the individual particles. Manipulation of the incoherent spectrum is often proposed as a mean to enhance stability; for example the increase of the betatron tune spread in accelerators by using nonlinear magnets [2]. In this paper we discuss a new mechanism for LD which occurs when the mode-particle coupling (MPC) has an extended frequency spectrum. This mechanism opens new possibilities for stability enhancement, via both particles' and the MPC's spectra manipulation.

The novel LD mechanism, which we call *parametric Landau damping*, is revealed by the numerical investigation of the transverse space charge (SC) modes in accelerator bunched beams at the coupling resonance (CR), *i.e.*, when the horizontal and the vertical tunes are close. In contrast with the usual LD mechanism, the frequency of the LD-responsible particles, *i.e.*, the particles which absorb the mode energy, have a wide spread and do not match the coherent frequency. This happens due to the modulation of the MPC by particle dependent oscillations with a wide frequency spread.

A common feature of the particles trapped in the vicinity of resonance fixed points is the oscillation of their amplitudes. In the CR case the trapped particles are characterized by an oscillatory energy exchange between the transverse planes. Their transverse amplitudes are oscillating with typical trapping frequencies. Since the MPC is dependent on the particles' amplitudes, it is modulated by the trapping frequency. The resonance condition for LD requires the particle frequency to equal the mode frequency shifted by the trapping frequency. Because the trapping frequencies are particle dependent, the frequencies of the LD-responsible particles may span a range equal to the one of the MPC frequency spectrum.

The transverse SC modes in bunched beams, away from the CR, were found analytically in Refs [3, 4]. Their intrinsic LD in the strong SC regime was suggested in Ref [3]. Predicted damping rates were confirmed by numerical simulations [5–7].

In our study the coupling between the transverse planes is produced by the SC force, thus no linear terms are present. The main resonance is the fourth-order Montague resonance [8] resulting from the term proportional to x^2y^2 in the SC potential.

We employ the Synergia accelerator modeling package [9, 10] to simulate the propagation of a single Gaussian beam through a linear lattice. The modes are extracted from the transverse displacement density using the dynamic mode decomposition (DMD) technique [11–14]. DMD is a data-driven algorithm used for modal analysis in both linear and nonlinear systems.

We compare the properties of the first SC mode both on and off the CR. We find that the LD is larger in the former case, while the frequency and the mode shape are nearly the same. By investigating the properties of the particles exchanging energy with the mode, we conclude that the off-resonance case well fits the conventional LD scenario characterized by LD-responsible particles with an incoherent frequency spectrum at the coherent frequency. At CR the damping enhancement is caused by the parametric LD mechanism, a consequence of the modulated coupling between the mode and the trapped particles. The existence of the parametric LD mechanism for the first SC mode at CR is proven solely by numerical simulations of a bunch propagating through a lattice; no analytical model is assumed.

Formalism We start by introducing parametric LD as a general mechanism and then proceed with discussing the specific example of transverse SC modes. The equation of motion for the particle i interacting with the mode \bar{x} can be written as

$$\ddot{x}_i + \omega_i^2 x_i = -K_i \bar{x}, \quad (1)$$

where x_i represents the particle displacement, ω_i the particle frequency, K_i the MPC and \bar{x} the collective mode. In systems with conventional LD, K is time independent or its oscillation frequency is particle independent.

The resonance condition is $\omega_i = \omega_c$, where ω_c is the $K\bar{x}$ frequency. The damping rate is proportional to the density of resonant frequencies, $\rho(\omega_c) = \sum_i \delta(\omega_i - \omega_c)$. For parametric LD mechanism, MPC is characterized by a frequency spectrum. If the frequency of $K_i(t)$ is μ_i , the resonance condition reads $\omega_i = \omega_c \pm \mu_i$. The damping rate is proportional to the MPC frequencies shifted density $h(\omega_c) = \sum_i \delta(\omega_c - \omega_i \pm \mu_i)$.

For transverse SC modes, Eq. 1 can be written as [15]

$$\ddot{x} + \omega_0^2 (Q_{0x} - \delta Q)^2 x = -2\omega_0^2 Q_{0x} \delta Q \bar{x}. \quad (2)$$

ω_0 is the angular revolution frequency and Q_{0x} is the bare betatron tune. The SC mode is $\bar{x}(t) = e^{-i\omega_0 \nu t} \bar{x}[z(t)]$, where ν is the mode tune. For the first mode, $\bar{x}[z] \approx \sin[\pi z/4\sigma_z]$ [3]. Taking into account the synchrotron oscillations of the longitudinal coordinate $z(t)$, the Bessel function expansion of $\bar{x}(t)$ yields the mode-particle main resonant exchange tune at $\nu - Q_s$, where Q_s is the synchrotron tune. $\delta Q(z, J_x, J_y)$ is proportional to the line charge density and is dependent on the particle transverse actions, J_x and J_y . In the off resonance case, to a good approximation, J_x and J_y are constants of motion. LD is conventional, since the MPC spectrum, resulting from the δQ dependence on $z(t)$ is particle independent.

The situation is different at the CR. In the proximity of the resonance, the sum $J_s = J_x + J_y$ is a constant of motion, while the difference $J_d = J_x - J_y$ oscillates around the stable point with the trapping frequency $\omega_0 Q_t$. Q_t is particle dependent [8]. Using the J_d expansion of the MPC term, $2\omega_0^2 Q_{0x} \delta Q = A + B J_d$, Eq. 2 can be written as

$$\ddot{x} + \omega_0^2 Q_x(z, J_s, J_d)^2 x = -A(z, J_s) \bar{x} - B(z, J_s) J_d \bar{x}. \quad (3)$$

The coupling term $A\bar{x}$ is conventional, while $B J_d \bar{x}$ yields parametric LD since it is modulated by Q_t . While in the former case the resonance condition is $\bar{Q}_x = \nu - Q_s$, the $B J_d \bar{x}$ term implies mode-resonant particles when $\bar{Q}_x = \nu - Q_s - Q_t$. Here \bar{Q}_x is the particle's main tune.

The oscillations of J_d contribute not only to the parametric LD but to the conventional one as well. The dependence of $Q_x(z, J_s, J_d)$ in Eq. 3 on J_d yields satellite features spaced by harmonics of Q_t in the incoherent spectrum. These satellites are resonant via $A\bar{x}$ coupling when their tune is equal to $\nu - Q_s$.

Simulations The simulations are done by employing the particle tracking code Synergia [9]. The SC effects are implemented using the second order split-operator method [16]. SC forces are calculated solving the 3D Poisson equation with open boundary conditions [17]. The bunch is initially excited in the horizontal plane with the first SC harmonic function. The excitation amplitude is small enough to ensure linear damping regime and not to affect the particles tune spectrum. The transverse displacement density, $X(z, \delta p/p, t)$ is calculated at every turn. The modes' shape, tune and damping are

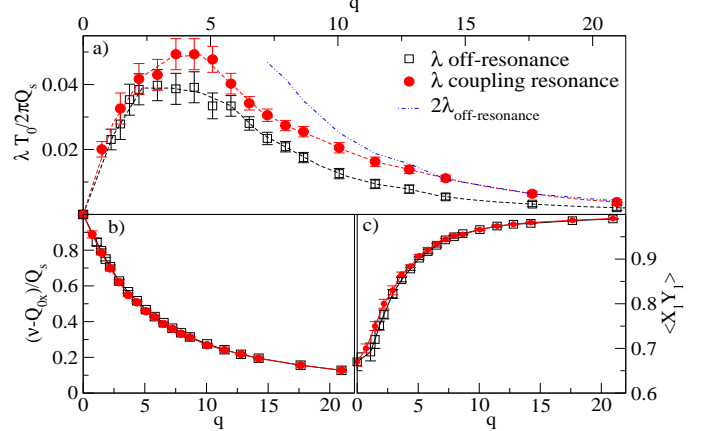


FIG. 1: Comparison between the off-resonance and the CR cases for the first SC mode: a) Landau damping rate (λ) vs. space charge parameter (q) at intermediate and strong SC showing the CR damping is larger. b) The mode tunes, ν , both off-resonance and at CR are nearly the same. c) The spatial overlap of the DMD extracted mode $X_1(z, u)$ with the SC harmonic function $Y_1(z)$. The off-resonance and CR mode shapes are nearly the same.

extracted from $X(z, \delta p/p, t)$ using the DMD technique. DMD [11–14] has been used for mode analysis in many fields such as fluid mechanics [18], neuroscience [19], and video streaming and pattern recognition [20]. Application of Synergia and DMD to beam dynamics is described in detail in [7].

A lattice made by 10 identical OFORODO (drift - focusing quad - drift - rf cavity - drift - defocusing quad - drift) cells is chosen. 10^8 macroparticles per bunch are used for the simulations. For the off-resonance case we take the bare betatron tune difference $Q_{0x} - Q_{0y} > \delta Q_{sc \ max}$ while at the CR $Q_{0x} = Q_{0y}$. $\delta Q_{sc \ max}$ is the SC tune shift at the center of the bunch. The chromaticity is zero. The beam distribution is longitudinally and transversely Gaussian with equal vertical and horizontal emittances. The SC parameter is defined as $q = \frac{\delta Q_{sc \ max}}{Q_s}$.

Results The properties of the first SC mode off-resonance and at CR are compared in Fig. 1. For intermediate and large SC, $q \gtrsim 4$, the damping at CR is larger, as shown in Fig. 1-a. In the strong SC regime, $10 \lesssim q \lesssim 20$, the damping at CR is larger by approximately a factor of 2. The relative enhancement increases slowly with q . However the precision of the simulation at large q is limited by the small value of the LD, which becomes of the order of the error bars. The mode tune measured relative to the bare betatron tune, $\nu - Q_{0x}$, is nearly the same for both cases, see Fig. 1-b. The difference between the mode spatial shape in the two cases is also insignificant, as illustrated in Fig. 1-c where the spatial overlap of the mode, $X_1(z, u)$, with the first SC

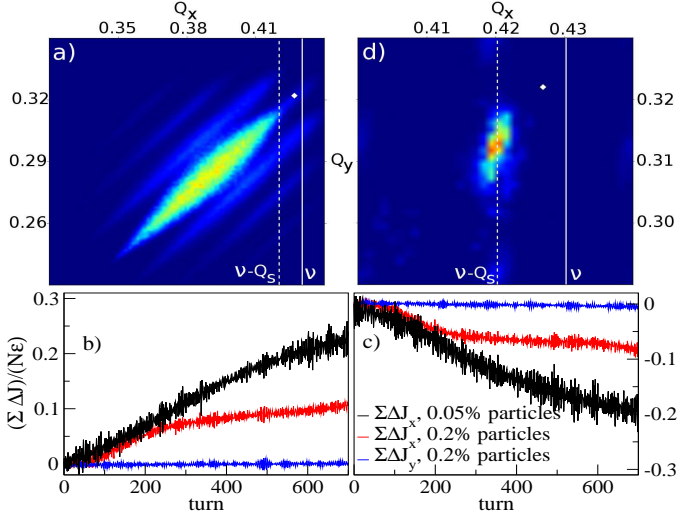


FIG. 2: a) Bunch tune footprint at off-resonance, $q = 7.94$. The white dot corresponds to the bare betatron tunes. b) $\sum_i \Delta J_x = \sum_i (J_{xi} - J_{xi \text{ initial}})$ and $\sum_i \Delta J_{yi} = \sum_i (J_{yi} - J_{yi \text{ initial}})$ of the 0.05% and 0.2% largest increasing energy particles versus turn number, normalized by the product of emittance and the number of the particles in the sum. c) The same as b) but for the largest decreasing energy particles. d) Tune footprint for the 0.5% largest changing energy (increase and decrease) particles. The tunes are in the proximity of the coherent tune $Q_x = \nu - Q_s$. The color dimension scale in a) and d) differs by one order of magnitude.

harmonic $Y_1(z)$ (calculated in [3]),

$$\langle X_1 Y_1 \rangle = \int X_1(z, u) Y_1(z) \rho(z, u) dz du, \quad (4)$$

is plotted.

The off-resonance LD mechanism can be understood within the typical paradigm. The beam 2D tune footprint, $\rho(Q_x, Q_y)$, is plotted in Fig. 2-a. $\rho(Q_x, Q_y)$ is defined as

$$\rho(Q_x, Q_y) = \sum_i |\tilde{x}_i(Q_x)|^2 |\tilde{y}_i(Q_y)|^2, \quad (5)$$

where $\tilde{x}_i(Q)$ ($\tilde{y}_i(Q)$) is the Fourier transform of the particle i horizontal (vertical) displacement $x_i(t)$ ($y_i(t)$). Since the LD is determined by the tune density and is insensitive to the particles' amplitude *per se*, we normalize the spectral weight of each particle to one. The SC force shifts the particles' tunes to lower values. The tune depression is maximal at the bunch center, while the particles in the distribution tails have a much smaller tune shift. The satellite lines separated by $2Q_s$ are a consequence of the modulation of the tune shift with the particle's longitudinal position. The particles directly responsible for the LD are the ones which resonantly exchange energy with the mode. To select the LD-responsible

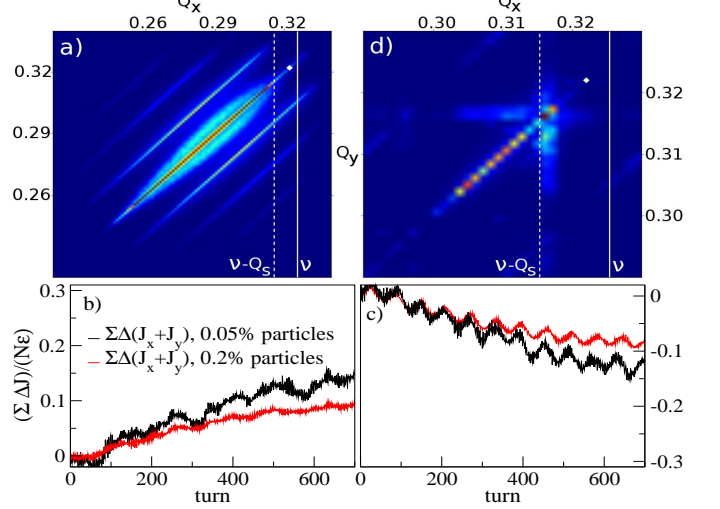


FIG. 3: a) Bunch tune footprint at CR, $q = 7.94$. The white dot corresponds to the bare betatron tunes. b) $\sum_i \Delta J_{si} = \sum_i (J_{si} - J_{si \text{ initial}})$ of the 0.05% and 0.2% largest increasing energy particles versus turn number, normalized by the product of emittance and the number of the particles in the sum. c) The same as b) but for the largest decreasing energy particles. d) Tune footprint for the 0.5% largest changing energy (increase and decrease) particles. Large part of the spectral weight is along the resonance line $2Q_x - 2Q_y = 0$, with the horizontal tune well below $\nu - Q_s$. The color dimension scale in a) and d) differs by one order of magnitude.

particles we look for those having the largest change in their energy during the simulation. In Fig. 2-b (-c) we plot the sum of $\Delta J_x = J_x - J_{x \text{ initial}}$ and the sum of $\Delta J_y = J_y - J_{y \text{ initial}}$ for the 0.05% and the 0.2% largest energy increase (decrease) particles. 0.05% and 0.2% are arbitrary chosen values for the purpose of illustrating the properties of the LD-responsible particles. In the linear LD theory, the energy of the LD-responsible particles increases linearly in a time interval $\delta t \approx 1/|\delta\omega|$, where $\delta\omega$ is the frequency difference between the particle and the mode. As seen from Fig. 2-b, the time where ΔJ_x is increasing linearly is larger when the number of the particles in the summation is smaller, since a larger number in the summation implies particles with larger $|\delta\omega|$. Note that the chosen particles increase or decrease their action only in the horizontal plane, *i.e.*, the plane where the mode is present. The 2D footprint of the 0.5% largest-energy-changing particles is shown in Fig. 2-d. As expected, since these particles are mode-resonant, their horizontal tune is in the vicinity of $\nu - Q_s$.

The spectral properties of the LD-responsible particles at the CR do not fit the typical LD paradigm. The beam 2D tune footprint in Fig. 3-a displays enhanced spectral weight along the coupling resonance line $2Q_x - 2Q_y = 0$,

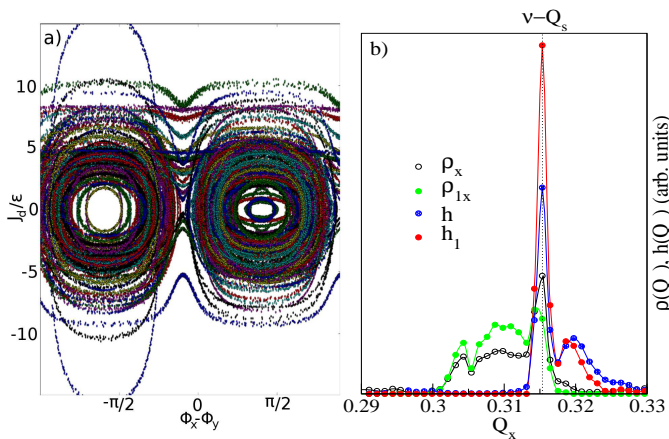


FIG. 4: Coupling resonance, $q = 7.94$. a) Poincare plots, J_d versus $\Phi_x - \Phi_y$, for randomly selected particles belonging to the 0.5% largest changing energy particles.

Most of these particles are trapped in the resonance islands. b) The horizontal tune density $\rho(Q_x)$ (black), the Q_t shifted tune density $h(Q_x)$ (blue) and the one-tune-per-particle tune density $\rho_1(Q_x)$ (green) with the corresponding Q_t shifted tune density $h_1(Q_x)$ for the 0.5% largest changing energy particles. $h(Q_x)$ and $h_1(Q_x)$ are strongly peaked at the resonant mode tune $Q_x = \nu - Q_s$, showing mode-particle resonance via the $B\bar{J}_d\bar{x}$ term.

consequence of resonance trapping. $2Q_s$ -spaced satellite lines can be observed. We use the same largest energy change criterion to select the LD-responsible particles. Unlike the off-resonance case, the horizontal and vertical actions exhibit non-monotonic change with turn number, since in the proximity of CR their magnitude oscillates between the planes. However, the transverse action sum J_s of the LD-responsible particles displays a monotonic increase (decrease), as shown in Fig. 3-b-(c). The interesting fact which points to a parametric damping mechanism is that the tune of most of these large energy changing particles is not in the vicinity of $\nu - Q_s$ as one would expect for LD-responsible particles. As shown in Fig. 3-d, there is a large spectral weight on the CR line which extends well below $Q_x = \nu - Q_s$.

Most of the large changing energy particles are trapped in resonance islands, as can be seen in Fig. 4-a where the Poincare plots, J_d versus $\Phi_x - \Phi_y$, are shown. The LD is, therefore, strongly influenced by the J_d oscillations characterizing the CR trapped particles.

The Q_t satellites in the particles' tune spectra contribute to the spectral weight at the mode coherent tune by $\approx 20\% \sim 25\%$. To estimate the satellites' spectral weight we compare the horizontal tune density $\rho_x(Q) = \sum_i \rho_{xi}(Q)$ and the one-tune-per-particle density $\rho_{1x}(Q) = \sum_i \rho_{1xi}(Q)$. The sum here is restricted

only to the number of the selected particles with the largest energy change. $\rho_{xi}(Q) = |\tilde{x}_i(Q)|^2$ and $\rho_{1xi}(Q) = \delta(Q - \bar{Q}_{xi})$. \bar{Q}_{xi} is the tune of the largest spectral peak in the Fourier spectrum $|\tilde{x}_i(Q)|$. Unlike ρ_x , where all spectral features are present, ρ_{1x} assumes that every particle is characterized only by its main tune. The spectral weight difference between ρ_x and ρ_{1x} at $\nu - Q_s$ measures the satellites contribution to the $A\bar{x}$ damping mechanism. ρ_x and ρ_{1x} for the 0.5% largest changing energy particles are shown in Fig. 4-b. Besides the peak at $\nu - Q_s$, in both ρ_x and ρ_{1x} a broad spectral feature at smaller frequency, unfavorable to the $A\bar{x}$ damping mechanism, is observed.

The other contribution of the J_d oscillations to the damping is via the $B\bar{J}_d\bar{x}$ term. The resonance condition is $Q_x + Q_t \approx \nu - Q_s$. We define $h(Q)$ as the tune density obtained by shifting each particle's horizontal tune by Q_t , such

$$h(Q) = \sum_i h_i(Q) = \sum_i \int \rho_{Jdi}(Q') \rho_{xi}(Q - Q') dQ' \quad (6)$$

$$\approx \sum_i \rho_{xi}(Q - Q_{ti}).$$

$\rho_{Jdi}(Q) = |\tilde{J}_{di}(Q)|^2$ is the particle's i J_d Fourier spectrum. $h_1(Q)$ is defined by replacing ρ_{xi} with ρ_{1xi} in Eq. 6. As shown in Fig. 4-b, both $h(Q)$ and $h_1(Q)$ are strongly peaked at the coherent frequency $\nu - Q_s$ and do not display the broad spectral feature seen in $\rho_x(Q)$ and $\rho_{1x}(Q)$ below $\nu - Q_s$. In fact the particles with the tune forming the broad spectral feature of $\rho_{1x}(Q)$ have the main tune $\bar{Q}_x \approx \nu - Q_s - Q_t$, *i.e.*, the tune required for resonance with the $B\bar{J}_d\bar{x}$ coupling term.

Compared to the off-resonance case, at CR the MPC term $B\bar{J}_d\bar{x}$ allows a larger number of particles to participate to the damping process. The conventional coupling does not favor particles with small longitudinal amplitudes, since they have a large tune shift which excludes them from the resonant exchange process with the mode. However, this impediment is not so restrictive for the resonant exchange via the $B\bar{J}_d\bar{x}$ term, since the trapping frequency Q_t is proportional to the charge density, thus also being large for small longitudinal amplitude particles and partially compensating for the large tune shift.

Conclusions A novel LD mechanism, driven by the modulation of the MPC is introduced. Numerical simulations using Synergia with the DMD method show the existence of this mechanism in bunched beams in the proximity of CR. The properties of the first SC mode are calculated for a Gaussian bunch propagating through an OFORODO lattice. The off-resonance and the CR cases are compared. While the SC mode's tune and shape are nearly the same, the LD is approximately a factor of 2 larger at CR in the strong SC regime. In the off-resonance case the damping mechanism can be understood within the conventional paradigm. The damping is caused by the resonant energy exchange between the mode and the particles with an incoherent tune equal to the mode's tune shifted by Q_s . At CR a large number

of particles are trapped around the stable points. Their transverse actions are oscillating with a particle dependent trapping frequency Q_t . The spectral properties of the trapped particles with large energy exchange reveal that their tune is additionally shifted from the mode's coherent tune by Q_t , supporting the parametric LD mechanism.

Acknowledgments This work was performed at Fermilab, operated by Fermi Research Alliance, LLC under Contract No. DE-AC02- 07CH11359 with the United States Department of Energy. Synergia development is partially supported through the ComPASS project, funded through the Scientific Discovery through Advanced Computing program in the DOE Office of High Energy Physics. An award of computer time was provided by the Innovative and Novel Computational Impact on Theory and Experiment (INCITE) program. This research used resources of the Argonne Leadership Computing Facility, which is a DOE Office of Science User Facility supported under Contract DE-AC02-06CH11357.

[1] L. Landau, “Oscillations of Electron Plasma”, *J. Phys. USSR*, **10**, 25 (1946).

[2] J. Gareyte, J.P. Koutchouk, F. Ruggiero (CERN), “Landau damping, dynamic aperture and octupoles in LHC”, CERN-LHC-PROJECT-REPORT-091, 1997.

[3] A. Burov, *PRST-AB* **12**, 044202 (2009); A. Burov, *PRST-AB* **12**, 109901(E), (2009).

[4] V. Balbekov, *PRST-AB* **12**, 124402 (2009).

[5] V. Kornilov and O. Boine-Frankenheim, *PRST-AB* **13**, 114201, (2010).

[6] V. Kornilov, *et al.*, “Thresholds of the head-tail instability in bunches with SC”, Proc. of HB2014 ICFA Workshop, East-Lansing, MI, USA (2014).

[7] A. Macridin, A. Burov, E. Stern, J. Amundson, and P. Spentzouris, *PRST-AB* **18**, 074401 (2015).

[8] B. W. Montague, CERN-Report No. 68-38, CERN, 1968.

[9] Synergia2, Accelerator Modeling, <https://cdcvns.fnal.gov/redmine/projects/synergia2/wiki>.

[10] J. Amundson, P. Spentzouris, J. Qiang, R. Ryne, *J. Comp. Phys.* **211**, 229 (2006).

[11] P.J. Schmid, *J. Fluid Mech.*, **656**, 5, (2010).

[12] C. W. Rowley, *et al.*, *J. Fluid Mech.*, **641**, 115, (2009).

[13] J. H. Tu, *et al.*, *Journal of Computational Dynamics*, **1**, 391, (2014).

[14] Kevin K. Chen, *et al.*, *Journal of Nonlinear Science* **22** Issue 6, 887, (2012).

[15] D. Mohl and H. Schonauer, Proc. IX Int. Conf. on High Energy Accelerators, Stanford, p. 380, (1974).

[16] H. Yoshida, *Phys. Lett. A* **150**, 262 (1990).

[17] R.W. Hockney and J. W. Eastwood, “Computer Simulation Using Particles”, McGraw-Hill (1981).

[18] See Ref [13] and the references therein.

[19] Bingni W. Brunton, *et al.*, *Journal of Neuroscience Methods*, Volume 258, p. 1 (2016).

[20] Jacob Grosek, *et al.*, arXiv:1404.7592, (2014).